Analytical Biochemistry
doi:10.1006/abio.2001.5137, available online at http://www.idealibrary.com on IDEAL®

A High-Throughput Screen for Identifying Transmembrane Pore-Forming Peptides

Joshua M. Rausch and William C. Wimley[1]
Department of Biochemistry SL43, Tulane University Health Sciences Center, New Orleans, Louisiana 70112-2699

Received February 7, 2001

We have developed a visual microwell plate assay for rapid, high-throughput screening for membrane-disrupting molecules such as *de novo* designed pore formers, antibiotic peptides, bacterial toxins, and lipases. The detectability is based on the strong fluorescence emission of the lanthanide metal terbium(III) (Tb^{3+}) when it interacts with the aromatic chelator dipicolinic acid (DPA). While Tb^{3+} is not strongly fluorescent alone, the binary complex emits bright green fluorescence when irradiated with uv light. For the microwell plate assay, we prepared unilamellar phospholipid vesicles that had either Tb^{3+} or DPA entrapped and the opposite molecule in the external solution. Disruption of the membranes allows the Tb^{3+}/DPA complex to form, giving rise to a visibly fluorescent solution. In plates with 20-μl wells, the lower limit of visual detectability of the Tb^{3+}/DPA complex in solution was about 2.5 μM. The lower limit of detectability using vesicles with entrapped Tb^{3+} or DPA was about 50 μM phospholipid. We show that the membrane-disrupting effect of as little as 0.25 μM or 5 pmol of the pore-forming, antibiotic peptide alamethicin can be detected visually with this system. This sensitive, high-throughput assay is readily automatable and makes possible the visual screening of combinatorial peptide libraries for members that permeabilize lipid bilayer membranes.

Key Words: **terbium; Tb^{3+}; dipicolinic acid; DPA; combinatorial; alamethicin.**

Control of the movement of molecules and information across biological membranes is an essential aspect of all living organisms. In part, this is why as many as one-third of all proteins are membrane proteins (1) and why half of all drugs are targeted to membrane-resident enzymes, channels, and receptors (2). The membrane is also the primary target for a wide range of natural polypeptide toxins (3–6) and antibiotics (7–10). Although diverse in sequence and structure, a unifying characteristic of these membrane-permeabilizing molecules is that they bind to target membranes as soluble monomers and then assemble into multimeric, membrane-spanning pores.

The *de novo* design and engineering of self-assembling, membrane-spanning protein pores could be important in such diverse fields as gene therapy, drug delivery, and antibiotic design. Membrane-spanning pores are also a key target for biosensor design (11) because they can be probed with techniques that have single-molecule sensitivity (12). Yet despite the potential importance of these classes of membrane-active polypeptides, our current level of understanding of the fundamental physical principles of folding and structure (13, 14) is not developed enough to drive their rational design and engineering. For this reason, structural biologists interested in designing membrane proteins would benefit from using combinatorial chemistry to achieve their biochemical engineering goals (15), as researchers have done for soluble molecules (16–18). However, the combinatorial design of membrane-resident molecules has not been emphasized because of the scarcity of effective screening assays. We present here a high-throughput, visual screening assay for membrane-spanning pores that is sensitive enough to screen combinatorial peptide libraries for members that assemble into pores in membranes. This assay is readily automatable and quantifiable and should be broadly useful in a variety of applications that focus on the ability of designed or natural molecules to form pores across lipid bilayer membranes.

MATERIALS AND METHODS

Materials

Terbium(III) chloride hexahydrate and dipicolinic acid (DPA)[2] were purchased from Molecular Probes

[1] To whom correspondence should be addressed. Fax: (504) 584-2739. E-mail: wwimley@tulane.edu.

[2] Abbreviations used: DPA, dipicolinic acid; POPC, palmitoyl oleoyl phosphatidylcholine.

0003-2697/01 $35.00

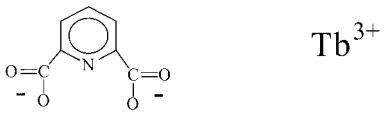

FIG. 1. Chemical structure of dipicolinic acid (DPA). Several molecules of DPA strongly chelate the lanthanide metal Tb^{3+} in solution giving rise to a fluorescent binary complex. This binary system is the basis for the screening assay described in this work.

(Eugene, OR). The chemical structure of DPA is shown in Fig. 1. Palmitoyl oleoyl phosphatidylcholine (POPC) was obtained from Avanti Polar Lipids (Alabaster, AL). Alamethicin was obtained from Sigma (St. Louis, MO). Throughout these experiments we used three isotonic buffers (19). All buffers contained 10 mM Tes and were titrated to pH 7 with KOH. The Tb^{3+}-containing buffer had 50 mM $TbCl_3$ and 85 mM Na_3 citrate; the DPA-containing buffer had 50 mM DPA and 200 mM NaCl. The final buffer solution, which was used to elute the vesicles from the gel filtration column, contained 290 mM NaCl.

Fluorescence Spectroscopy

Fluorescence spectroscopy was performed with an SLM-Amino Model 8100 spectrofluorometer. Excitation was at 270 nm and emission was measured between 350 and 600 nm. Monochrometer slitwidths were 8 nm and the intensities were measured as a ratio of emission intensity to the lamp intensity. Glann–Thompson polarizers were used in the magic angle configuration to reduce the effects of light scattering from vesicle solutions (20).

Preparation of Vesicles with Entrapped Tb^{3+} or DPA

To encapsulate Tb^{3+} or DPA in vesicles, a lipid suspension was prepared by adding the appropriate amount of POPC in chloroform to a glass tube, drying under vacuum for 6 h, and then adding enough buffer to bring the concentration to 100 mM total lipid. The buffer contained 50 mM Tb^{3+}, 50 mM DPA, or an equivalent amount of NaCl. The lipid suspension was frozen and thawed 10 times to ensure the distribution of the indicator molecules between the interior and exterior of the vesicles (21). Unilamellar vesicles were made by extrusion under high pressure through two stacked Nucleopore polycarbonate filters with 0.1-μm-diameter pores (22, 23). This process produces uniformly sized, unilamellar vesicles of 0.1 μm diameter (22, 23). Removal of the external Tb^{3+} or DPA was accomplished by eluting aliquots of the vesicles over a 1 $\times$ 25-cm Sephadex G-75 gel filtration column using a buffer that was made isotonic to the entrapped solution by replacing the Tb^{3+}/DPA with NaCl. DPA-containing vesicles retained a small amount of external DPA after the first elution and therefore had to be run over the column a second time to completely remove the external DPA. Once prepared, the internal contents of these vesicles were retained for at least several months when the vesicles were stored at 5°C.

Microwell Plate Assay

For the microwell plate assay a 20-μl aliquot of vesicle solution was pipetted into each well of plastic 10 $\times$ 6 format plate. The volume of the wells was smaller than 20 μl; therefore, the test solutions formed a dome-shaped drop in the well. Volumes as small as 5 μl can easily be used in this assay system. Alamethicin or Triton X-100 was added from concentrated stock solutions and the well contents were mixed with pipette tip aspiration. Except where noted, the vesicles were present at 200 μM and had entrapped Tb^{3+} at $\sim$10 μM total concentration and external DPA at 50 μM. In every experiment, we directly compared the Tb^{3+}/DPA fluorescence of the test wells to that of wells containing the same amount of untreated vesicles and to wells containing vesicles that has been lysed with the detergent Triton-X-100. The microwell plate was examined visually in a darkroom under short-wave uv illumination. Under these condition wells with Triton X-100-lysed vesicles give bright green fluorescence while untreated vesicles are indistinguishable from buffer-only or lipid-only background.

Photography

The images in Figs. 3–5 were obtained photographically on Kodak Royal Gold ASA400 color film using a vertically mounted Minolta X-700 SLR camera fitted with a f3.6 50-mm macro lens. No optical filters were used. Oblique illumination was obtained with a horizontally mounted short-wave uv light source, nominally 254 nm, in a darkroom. Exposure times were 4 s and film development was done by standard commercial methods. Photos were scanned with a digital scanner at 400 dpi resolution in gray-scale mode. Color images are available from the authors upon request. The only image manipulation applied was a global adjustment of the brightness and contrast during the image scanning process. The visual detectability of the lowest intensity samples was better than the photographic detectability in the figures.

RESULTS AND DISCUSSION

The Binary Terbium/Dipicolinic Acid System

The usefulness of the strong fluorescence of chelated lanthanides in membrane studies was first illustrated in an assay for compartment mixing in vesicle fusion studies (19). The fluorescence, or luminescence, of terbium and other lanthanides is due to the electronic transitions of the *f*-orbital electrons. This is why the emission bands, shown in Fig. 2, are narrow and show

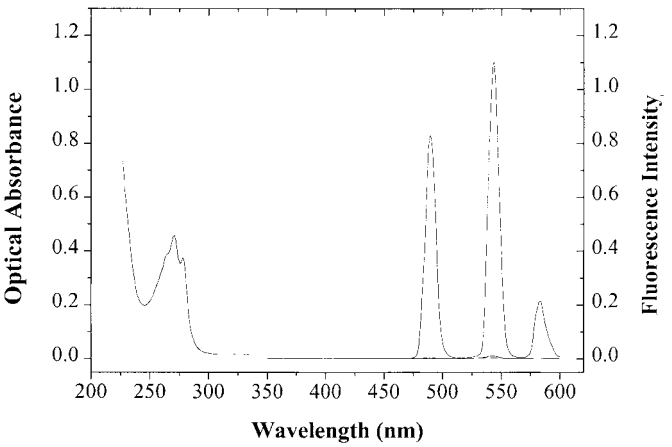

FIG. 2. Optical absorbance (left) and fluorescence emission (right) of Tb^{3+} chelated with an excess of dipicolinic acid. The absorbance of the Tb^{3+}/DPA complex is nearly identical to that of DPA alone (not shown). At the right is the bright fluorescence of the Tb^{3+}/DPA complex. For comparison we also show the fluorescence of Tb^{3+} alone as a curve that is barely distinguishable from the buffer baseline.

electronic fine structure in their distribution. Although many chelators enhance Tb^{3+} fluorescence, one of the brightest conjugates is made from Tb^{3+} and the membrane-impermeant aromatic chelator DPA (19) (Fig. 1). The complex has an absorbance maximum, due to the DPA molecule, at around 270 nm. The enhancement of terbium fluorescence by DPA is due to energy transfer from the aromatic ring. In Fig. 2 we show the sharp emission bands of Tb^{3+}/DPA at 490, 545, and 585 nm. There are several weaker, long-wavelength bands that are not shown in Fig. 2

In aqueous experiments, terbium is solubilized by chelating it with citrate (19), a tricarboxylic acid. The fluorescence of the Tb^{3+}/citrate complex is very low. Citrate is a much weaker Tb^{3+} chelator than DPA and is readily displaced when DPA is present. In the presence of DPA, Tb^{3+} is chelated by three molecules (24) with a dissociation constant that is smaller than the concentrations that we utilized in these studies (>2 μM). Spectroscopic measurements and competition experiments (24) have shown that the first two DPA molecules in the conjugate give rise to most of the fluorescence enhancement. Consistent with this observation, a Hill coefficient of 1.6 was reported for DPA dependence of Tb^{3+} fluorescence (24). Throughout the studies reported here we used a DPA to Tb^{3+} ratio of at least 3. The addition of excess DPA does not change the fluorescence intensity in any concentration range we tested. These observations are important because it means that we can perform this screening assay in solutions containing as little as 10 μM Tb^{3+} or DPA, thus reducing the probability that the indicator molecules will interfere with any other component of a system being tested.

Limits of Detectability

The visual detectability of the Tb^{3+}/DPA complex in solution was assessed using dilute solutions at concentrations between 1 and 100 μM Tb^{3+} with a threefold excess of DPA. Wells in micro plates were filled with 20 μl of either buffer or Tb^{3+}/DPA solution and were visually examined in a darkroom under short-wave (254-nm) uv illumination. At these concentrations citrate-chelated Tb^{3+} or DPA alone were indistinguishable from buffer and had no visible fluorescence. Citrate–Tb^{3+} is visibly fluorescent only in the millimolar concentration range whereas solutions of Tb^{3+} and DPA have bright green fluorescence in the micromolar concentration range. A gray-scale image of an example plate is shown in Fig. 3. The lower limit of visual detectability in this microplate format was approximately 2.5 μM (or 50 pmol) of Tb^{3+} in a 20 μl well. Importantly, in the microwell plate assay the range over which there was a noticeable dependence of visible fluorescence on total Tb^{3+}/DPA concentration was from about 2.5 to about 100 μM.

Terbium and DPA Encapsulation in Lipid Vesicles

Unilamellar lipid vesicles with an outer diameter of 0.1 μM were prepared by extrusion (22, 23) from POPC as described above. Initial concentrations were 100 mM POPC and 50 mM Tb^{3+} or DPA. Maximal trapped volumes in this type of vesicle are 1.5–2 μl per micromole of lipid (25). We expected, for 100 mM POPC that the concentration of entrapped indicator would be at most 10% of the lipid concentration. Fluorescence measurements indicated that the trapped volume in our vesicles was about 1 μl per micromole of lipid or about 5% of the lipid concentration. The removal of external Tb^{3+} or DPA was confirmed by fluorescence measurements. Further experiments also demonstrated that the spontaneous permeation of Tb^{3+} and DPA across the POPC bilayers did not occur to a measurable extent at neutral pH for up to several months after the vesicles were prepared.

At lower pH values, the weak aromatic acid DPA was expected to permeate membranes more rapidly. The useful pH range of the assay was determined by visually examining the fluorescence of vesicle solutions with entrapped Tb^{3+} and external DPA at pH values between 3 and 10. At pH 3, the separation of external DPA and entrapped Tb^{3+} is lost almost instantly, giving brightly fluorescent solutions in the absence of membrane-disrupting molecules. At pH 3.5 the untreated vesicles are fluorescent within 10–15 min. However, at pH 4, the separation of external DPA and internal Tb^{3+} is maintained for an experimentally useful time of about 1 h. At high pH, the assay is limited by the alkaline hydrolysis of the phospholipids. Thus, the useful pH range of this assay is from pH 4.0 to pH 10.0, with experimental stability of internal/external

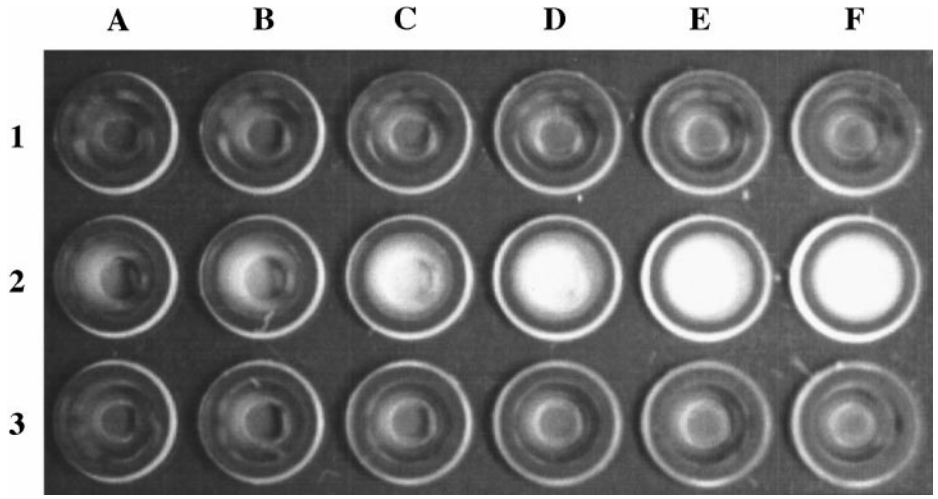

FIG. 3. Visual detectability of Tb^{3+}/DPA fluorescence in microwell plates. Plates contained 20 μl of solution in each well. For comparison, all the wells in rows 1 and 3 contain 20 μl of buffer. In row 2 the Tb^{3+} concentrations are, from A to F: 1, 2, 4, 6, 8, and 10 μM Tb^{3+}. Each Tb^{3+}-containing sample has a threefold molar excess of DPA. Solutions of Tb^{3+} or DPA alone were indistinguishable from buffer. Wells are 2 mm in diameter.

separation ranging from 1 h at the extremes of pH to months at neutral pH. We are currently investigating the properties of other binary fluorophore systems to be used for extending the useful pH range of this assay to lower pH conditions.

Microplate Assay—Limit of Vesicle Detectability

The limit of detectability in the vesicle assay was assessed with a 200 μM stock vesicle solution that contained ~10 μM entrapped Tb^{3+} and 50 μM external DPA. This solution was diluted into 20 μl wells to give final concentrations between 20 and 200 μM. An example plate is shown in Fig. 4. The fluorescence was assessed visually in a darkroom under short-wave (254-nm) uv illumination. Wells containing as little as 50 μM (2 nmol) of lysed vesicles are readily distinguished from buffer or untreated vesicles, which are indistinguishable from each other. We used a concentration of 200 μM lipid in all subsequent screening experiments.

Detection of Pore-Forming Peptides

This screening assay has many potential uses, but it was specifically designed to screen combinatorial peptide libraries for molecules that permeabilize membranes by assembling into membrane-spanning pores

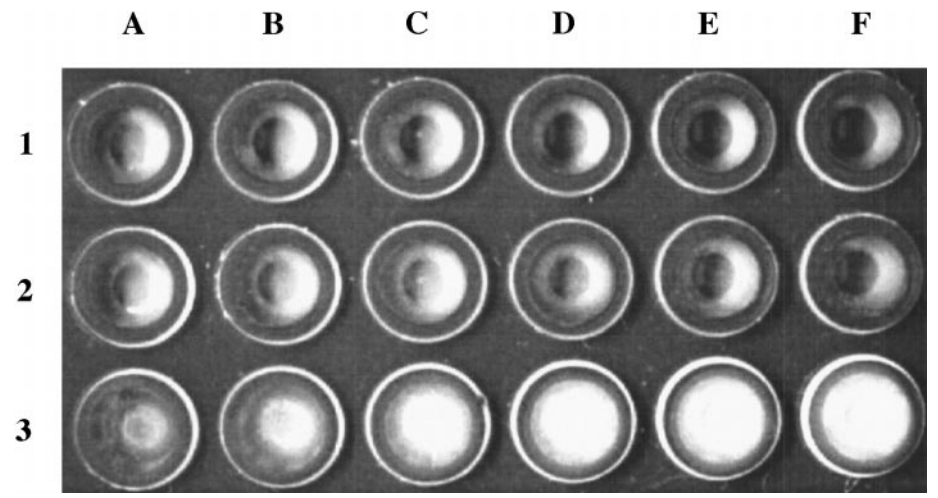

FIG. 4. Visual detectability of vesicles with entrapped Tb^{3+} and an excess of external DPA. All three rows contain 20 μl of POPC vesicles at the following concentrations, from A to F: 20, 40, 80, 120, 160, and 200 μM. Row 1 contains vesicles that do not contain Tb^{3+} or DPA. The wells in row 2 contain unlysed vesicles with entrapped Tb^{3+} and external DPA. The wells in row 3 contain vesicles with entrapped Tb^{3+} and external DPA that have been lysed with 1 μl of 10% Triton X-100. Wells are 2 mm in diameter.

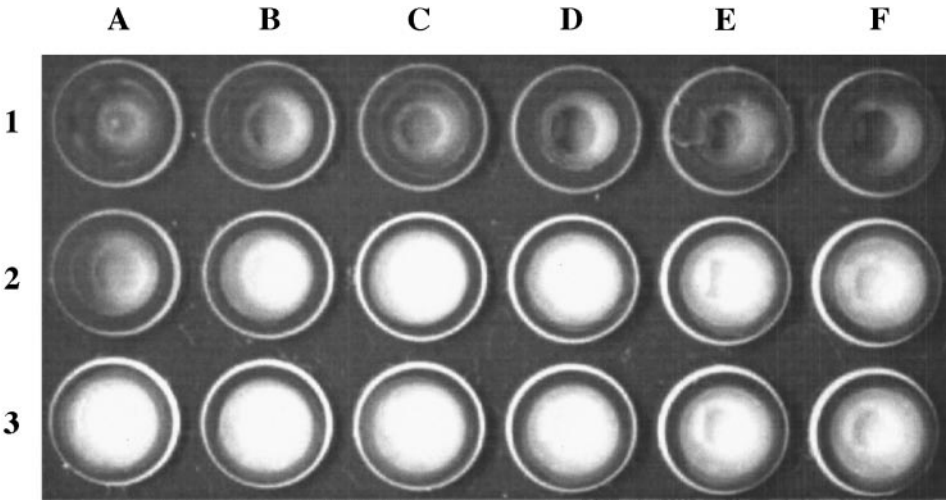

FIG. 5. Sensitivity of the vesicle permeabilization assay to release caused by the pore-forming, antimicrobial peptide alamethicin. Each well in this plate contains 20 μl of a 200 μM solution of POPC vesicles with entrapped Tb^{3+} and external DPA. Wells in the first row were untreated. Wells in the second row contained the following amounts of alamethicin, from A to F: 0.125, 0.25, 0.5, 1, 2, and 4 μM. The vesicles in the third row have been completely lysed with 1 μl of 10% Triton X-100. Wells are 2 mm in diameter.

or channels. Many membrane-permeabilizing peptides are active in the range between 1/30 and 1/500 peptides per lipid (26–28), although some are active at ratios (29) as low as 1/10,000. Thus, based on the detectability limits established above, we expect to be able to detect pore formation caused by less than 0.5 μM (10 pmol) of peptide. To test the sensitivity of our assay, we used the fungal antibiotic peptide alamethicin (30) which is known to permeabilize vesicles by assembling into multimeric pores at concentrations of one peptide per several hundred lipids (28). In the experimental tests we used a lipid concentration of 200 μM vesicles in all wells and added increasing amounts of alamethicin from a stock solution. The results were the same whether we used vesicles with internal Tb^{3+} and external DPA or vesicles with internal DPA and external Tb^{3+}. An example plate is shown in Fig. 5 in which we tested the effect of alamethicin on vesicles with internal Tb^{3+} and external DPA. We tested alamethicin concentrations between 0.125 and 2 μM peptide. Alamethicin concentrations of 1 μM (or 20 pmol) or higher instantly permeabilized the vesicles, giving Tb^{3+}/DPA fluorescence equal to that of detergent-solubilized vesicles (see Fig. 5). Alamethicin concentrations between 0.25 and 1 μM caused slower release. At 0.25 μM alamethicin the full effect required 10 min to complete but the fluorescence eventually reached the maximal intensity. Alamethicin concentrations below 0.25 μM only slightly increased the fluorescence of the vesicle solutions in the microwell plate, even after a 1-h-long incubation. We conclude that for our test peptide, alamethicin, the limit of easy visual detectability is approximately 0.25 μM, which is equivalent to 5 pmol or about 10 ng of peptide.

Usefulness for Combinatorial Peptide Libraries

We showed above that we can readily detect the membrane permeabilization caused by as little as 5 pmol of the peptide alamethicin. Importantly, this is less than 1/10 of the amount of peptide that is present on a *single* resin bead of the type typically used for solid-phase peptide synthesis (31). Therefore this high-throughput assay is very well suited for screening combinatorial libraries of peptides for members that form pores in membranes. For example, this assay can be used to screen peptide libraries synthesized by the split-and-recombine method (32). In a split-and-recombine synthesis, the solid-phase resin, which contains about 10^6 spherical polymer beads per gram of resin, is split into batches at each combinatorial position. Each batch of resin is coupled with one particular amino acid and the beads are then recombined and mixed before the next splitting step. By this method each 100- to 150-μm resin bead will have coupled to it about 100 pmol ($\sim$200 ng) of the same sequence, but every bead in the library will contain a different sequence. Using our microplate assay, in conjunction with photolabile peptide-bead linkers and microsequencing (33) it is now possible to screen large combinatorial libraries for individual sequences that assemble into pores in membranes. This assay is also useful for screening peptide libraries synthesized by other methods such as the multipin (34) or SPOT synthesis (35) methods.

CONCLUSIONS

Structural biologists are increasingly turning to combinatorial methods to achieve their biochemical engineering goals (16–18). While there are many useful

screening methods for soluble molecules and a few for membrane-resident molecules (15), the combinatorial design of membrane-active molecules has been inhibited by the paucity of good high-throughput screens. In the work presented here, we have described a very sensitive, automatable, high-throughput, visual screen for molecules that permeabilize lipid bilayer membranes.

ACKNOWLEDGMENT

Work was supported by NIH (GM60000).

REFERENCES

1. Wallin, E., and von Heijne, G. (1998) Genome-wide analysis of integral membrane proteins from eubacterial, archaean, and eukaryotic organisms. *Protein Sci.* **7,** 1029–1038.
2. Drews, J. (2000) Drug discovery: A historical perspective. *J. Biomol. Struct. Dyn.* **287,** 1960–1964.
3. Shatursky, O., Heuck, A. P., Shepard, L. A., Rossjohn, J., Parker, M. W., Johnson, A. E., and Tweten, R. K. (1999) The mechanism of membrane insertion for a cholesterol-dependent cytolysin: A novel paradigm for pore-forming toxins. *Cell* **99,** 293–299.
4. Bayley, H. (1997) Toxin structure: Part of a hole? *Curr. Biol.* **7,** R763–R767.
5. Pugsley, A. P. (1996) Bacterial toxins deliver the goods. *Proc. Natl. Acad. Sci. USA* **93,** 8155–8156.
6. Schneider, E., Haest, C. W. M., Plasa, G., and Deuticke, B. (1986) Bacterial cytotoxins, amphotericin B and local anesthetics enhance transbilayer mobility of phospholipids in erythrocyte membranes: Consequences for phospholipid asymmetry. *Biochim. Biophys. Acta* **855,** 325–336.
7. White, S. H., Wimley, W. C., and Selsted, M. E. (1995) Structure, function, and membrane integration of defensins. *Cur. Opin. Struct. Biol.* **5,** 521–527.
8. Selsted, M. E., Tang, Y. Q., Morris, W. L., McGuire, P. A., Novotny, M. J., Smith, W., Henschen, A. H., and Cullor, J. S. (1993) Purification, primary structures, and antimicrobial activities of β-defensins, a new family of antimicrobial peptides from bovine neutrophils. *J. Biol. Chem.* **268,** 6641–6648.
9. Bechinger, B. (1997) Structure and functions of channel-forming peptides: Magainins, cecropins, melittin and alamethicin. *J. Membr. Biol.* **156,** 197–211.
10. Maloy, W. L., and Kari, U. P. (1995) Structure–activity studies on magainins and other host defense peptides. *Biopolymers* **37,** 105–122.
11. Bayley, H. (1999) Designed membrane channels and pores. *Curr. Opin. Biotechnol.* **10,** 94–103.
12. Neher, E., Sakmann, B., and Steinbach, J. H. (1978) The extracellular patch clamp: A method for resolving currents through individual open channels in biological membranes. *Pflugers Arch.* **375,** 219–228.
13. White, S. H., and Wimley, W. C. (1999) Membrane protein folding and stability: physical principles. *Annu. Rev. Biophys. Biomol. Struct.* **28,** 319–365.
14. Popot, J. L., and Engelman, D. M. (2000) Helical membrane protein folding, stability, and evolution. *Annu. Rev. Biochem.* **69,** 881–922.
15. Russ, W. P., and Engelman, D. M. (1999) TOXCAT: A measure of transmembrane helix association in a biological membrane. *Proc. Natl. Acad. Sci. USA* **96,** 863–868.
16. Blondelle, S. E., Takahashi, E., Houghten, R. A., and Pérez-Payá, E. (1998) Rapid identification of compounds with enhanced antimicrobial activity by using conformationally defined combinatorial libraries. *Biochem. J.* **313,** 141–147.
17. Gu, H., Yi, Q., Bray, S. T., Riddle, D. S., Shiau, A. K., and Baker, D. (1995) A phage display system for studying the sequence determinants of protein folding. *Protein Sci.* **4,** 1108–1117.
18. al Obeidi, F. A., and Lam, K. S. (2000) Development of inhibitors for protein tyrosine kinases. *Oncogene* **19,** 5690–5701.
19. Wilschut, J., and Papahadjopoulos, D. (1979) Ca2+-induced fusion of phospholipid vesicles monitored by mixing of aqueous contents. *Nature* **281,** 690–692.
20. Ladokhin, A. S., Jayasinghe, S., and White, S. H. (2000) How to measure and analyze tryptophan fluorescence in membranes properly, and why bother? *Anal. Biochem.* **285,** 235–245.
21. Hope, M. J., Bally, M. B., Mayer, L. D., Janoff, A. S., and Cullis, P. R. (1986) Generation of multilamellar and unilamellar phospholipid vesicles. *Chem. Phys. Lipids* **40,** 89–109.
22. Nayar, R., Hope, M. J., and Cullis, P. R. (1989) Generation of large unilamellar vesicles from long-chain saturated phosphatidylcholines by extrusion technique. *Biochim. Biophys. Acta* **986,** 200–206.
23. Mayer, L. D., Hope, M. J., and Cullis, P. R. (1986) Vesicles of variable sizes produced by a rapid extrusion procedure. *Biochim. Biophys. Acta* **858,** 161–168.
24. Sanny, C. G., and Price, J. A. (1999) Analysis of nonlinear quenching of terbium(III):dipicolinic acid complex fluorescence by chelators and chelate-conjugated macromolecules. *Bioconjug. Chem.* **10,** 141–145.
25. Wu, H., Zheng, L., and Lentz, B. R. (1996) A slight asymmetry in the transbilayer distribution of lysophosphatidylcholine alters the surface properties and poly(ethylene glycol)-mediated fusion of dipalmitoylphosphatidylcholine large unilamellar vesicles. *Biochemistry* **35,** 12602–12611.
26. Wimley, W. C., Selsted, M. E., and White, S. H. (1994) Interactions between human defensins and lipid bilayers: Evidence for the formation of multimeric pores. *Protein Sci.* **3,** 1362–1373.
27. Grant, E., Beeler, T. J., Taylor, K. M. P., Gable, K., and Roseman, M. A. (1992) Mechanism of magainin-2a induced permeabilization of phospholipid vesicles. *Biochemistry* **31,** 9912–9918.
28. Fringeli, U. P., and Fringeli, M. (1979) Pore formation in lipid membranes by alamethicin. *Proc. Natl. Acad. Sci. USA* **76,** 3852–3856.
29. Parente, R. A., Nir, S., and Szoka, F. (1990) Mechanism of leakage of phospholipid vesicle contents induced by the peptide GALA. *Biochemistry* **29,** 8720–8728.
30. Cafiso, D. S. (1994) Alamethicin: A peptide model for voltage gating and protein–membrane interactions. *Annu. Rev. Biophys. Biomol. Struct.* **23,** 141–165.
31. Merrifield, R. B. (1969) Solid-phase peptide synthesis. *Adv. Enzymol. Relat. Areas Mol. Biol.* **32,** 221–296.
32. Furka, A., and Bennett, W. D. (1999) Combinatorial libraries by portioning and mixing. *Comb. Chem. High Throughput Screen.* **2,** 105–122.
33. Stolowitz, M. L. (1993) Chemical protein sequencing and amino acid analysis. *Curr. Opin. Biotechnol.* **4,** 9–13.
34. Maeji, N. J., Bray, A. M., and Geysen, H. M. (1990) Multi-pin peptide synthesis strategy for T cell determinant analysis. *J. Immunol. Methods* **134,** 23–33.
35. Frank, R., and Overwin, H. (1996) SPOT synthesis: Epitope analysis with arrays of synthetic peptides prepared on cellulose membranes. *Methods Mol. Biol.* **66,** 149–169.